RSC Advances

PAPER

View Article Online
View Journal | View Issue

Cite this: *RSC Adv.*, 2014, **4**, 15740

Melting temperatures deduced from molar volumes: a consequence of the combination of enthalpy/entropy compensation with linear cohesive free-energy densities†

Thibault Dutronc,* Emmanuel Terazzi* and Claude Piguet*

Enthalpy/entropy compensation is a general issue of intermolecular binding processes when the interaction between the partners can be roughly modelled with a single harmonic potential. Whereas linear *H*/*S* correlations are wished for by experimentalists, and often graphically justified, no inflexible law of thermodynamics supports the latter statement. On the contrary, the non-directional Ford's approach suggests logarithmic *H*/*S* relationships, which can be linearized only over narrow enthalpy/entropy ranges. Predictions covering larger domains require mathematical mapping obeying specific boundary conditions which are not compatible with linear plots. The analysis of solvent-free melting processes operating in six different classes of organic and inorganic materials shows that reciprocal Hill plots are acceptable functions for correlating melting enthalpies and entropies. The combination of *H*/*S* compensation with the observed linear dependence of the cohesive free energy densities with respect to the melting temperature eventually provides an unprecedented interdependence between melting temperatures and molar volumes. This procedure is exploited for the prediction of melting temperatures in substituted cyanobiphenyls.

Received 13th January 2014
Accepted 18th March 2014

DOI: 10.1039/c4ra00348a

www.rsc.org/advances

Introduction

A rational control and programming of the various contributions to the changes in standard thermodynamic free energy ΔG^0_{asso}, enthalpy ΔH^0_{asso} and entropy ΔS^0_{asso} of association accompanying the binding process depicted in eqn (1) is at the heart of self-assemblies occurring in biology,[1] in physics[2] and in chemistry[3] (|| refers to the activities of various partners).

$$A + B \rightleftarrows [AB] \quad \Delta G^0_{asso} = \Delta H^0_{asso} - T\Delta S^0_{asso} = -RT \ln\left(\frac{|[AB]|}{|A||B|}\right) \tag{1}$$

Beyond the theoretically justified Gibbs free energy relationship (eqn (1), right-hand side),[4] the simple modelling of the interaction operating between the partners in the [AB] pair by using a harmonic potential (*i.e.* a spring) suggests that the stronger the binding energy (measured as the potential well depth $u_{min} \propto \Delta H^0_{asso}$), the larger its force constant κ (measured as its mean vibrational frequency $\nu = (1/2\pi)\sqrt{\kappa/m_r} \propto -\Delta S^0_{asso}$ where m_r is the reduced mass of the harmonic oscillator).[5]

Consequently, enthalpy and entropy changes are usually correlated for a simple intermolecular binding event with a propensity for compensation, *i.e.* ΔS^0_{asso} and ΔH^0_{asso} concomitantly decrease or increase.[6] Recurrent, but empirical observations collected from series of association processes investigated in biology, in physics and in chemistry show that minor structural perturbations of the two partners lead to apparent linear correlations (eqn (2), left-hand side). The slope α of the ΔH_i *versus* ΔS_i plot has Kelvin units and is often referred to as the compensation temperature T^{comp}, *i.e.* the temperature at which all association processes *i* within a homogeneous series display the same compensation free energy change $\Delta G^{comp} = \gamma$ (eqn (2), center). Its re-writing at the right-hand side of eqn (2) is reminiscent of the Gibbs relationship, which may explain the rather common belief in the statement that linear enthalpy/entropy compensation corresponds to a 'fourth law' of thermodynamics.[6,7]

$$\Delta H_i = \alpha\Delta S_i + \gamma = T^{comp}\Delta S_i + \Delta G^{comp} \Rightarrow \Delta G^{comp} = \Delta H_i - T^{comp}\Delta S_i \tag{2}$$

Theoretical approaches based on statistical thermodynamics include both attempts to refute the relevance of enthalpy–entropy correlation,[8] as well as to establish its signature as the result of (i) minor perturbations of equilibrium constants,[9] (ii) partition functions governed by a Gaussian density of states[6b] or (iii) underlying hidden thermodynamic processes.[6c] In 2005,

Department of Inorganic and Analytical Chemistry, University of Geneva, 30 quai E. Ansermet, CH-1211 Geneva 4, Switzerland. E-mail: Claude.Piguet@unige.ch; Emmanuel.Terazzi@unige.ch; Thibault.Dutronc@unige.ch

† Electronic supplementary information (ESI) available. See DOI: 10.1039/c4ra00348a

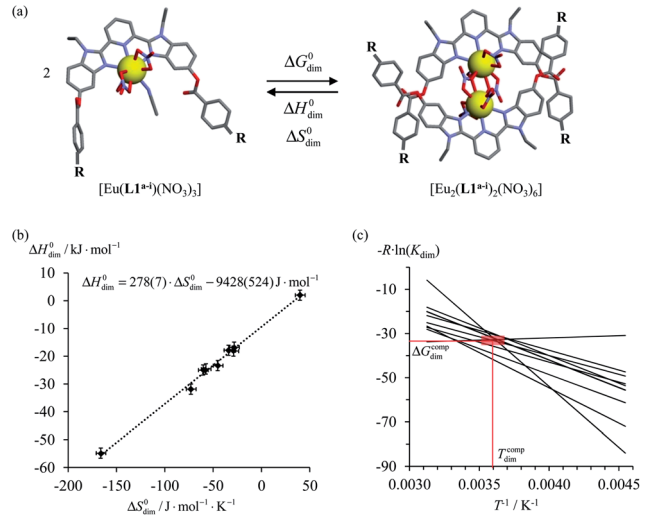

Fig. 1 (a) Schematic dimerization of complexes $[Eu(L1^{a-i})(NO_3)_3]$ occurring in dichloromethane, (b) associated "linear" ΔH^0_{dim} *vs.* ΔS^0_{dim} plots and (c) individual van't Hoff $\Delta G_{dim}/T$ *vs.* T^{-1} plots for nine different *R* substituents.[13]

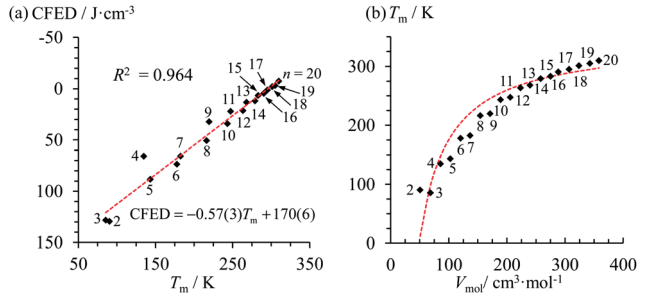

Fig. 2 Plots of (a) the cohesive free energy densities (CFED) *versus* the melting temperature (T_m) and (b) the melting temperature (T_m) *versus* the molar volumes (V_{mol}) for saturated linear hydrocarbons C_nH_{2n+2} (n = 2–20). The dotted red traces show the theoretical curves. Adapted from ref. 17.

Ford derived a non-quantum justification (see next section) claiming that enthalpy/entropy compensation ($T^{comp} > 0$ in eqn (2)) occurs when the minimum host–guest separation r_0 in the $[AB]_i$ pairs remains constant within a series of intermolecular binding events.[10] However, the linearity proposed in eqn (2) does not result from Ford's model,[6d] and alternative physical justifications for parabolic[5a,11] or rectangular-hyperbolic[12] correlation for *H*/*S* compensation have been proposed. In this context, Liu and Guo documented that the general emergence of linear *H*/*S* compensation is often the consequence of statistical and mathematical artefacts arising from the data analysis.[6a] The dimerization process depicted in Fig. 1a illustrates this statement since the convincing linear relationship found for *H*/*S* compensation (Fig. 1b) is significantly discredited when one considers the alternative, but equivalent van't Hoff plots which should cross at a common $\langle T^{comp}; \Delta G^{comp} \rangle$ couple (red rectangle in Fig. 1c).[13]

Since complexation processes occurring in dilute solutions are complicated by unavoidable solvation changes,[11,14] which may induce additional *H*/*S* compensation phenomenon,[15] we resorted to the melting of solids into isotropic liquid conducted in absence of solvents or of additives for getting a rough estimation of the strength of the intermolecular interactions occurring in a solid.[16] These processes can be idealized as reversible n^{th} order chemical reactions, in which n identical monomeric units A associate into fully assembled entities A_n (eqn (3)).[17]

$$n\mathrm{A} \underset{\Delta G^0_m = \Delta H^0_m - T\Delta S^0_m}{\overset{\Delta G^0_{asso} = \Delta H^0_{asso} - T\Delta S^0_{asso}}{\rightleftharpoons}} \mathrm{A}_n \qquad (3)$$

At the melting temperature $T = T_m$, the solid–liquid phase equilibrium implies that $\Delta G_{asso} = \Delta G_m = 0$ and $T_m = \Delta H^0_m/\Delta S^0_m = \Delta H^0_{asso}/\Delta S^0_{asso} = \Delta H_m/\Delta S_m$ when one reasonably assumes that the melting enthalpies ΔH_m and entropies ΔS_m operating at the melting temperatures are satisfyingly estimated by those defined in the standard conditions (*i.e.* $\Delta H_m \approx \Delta H^0_m$ and $\Delta S_m \approx \Delta S^0_m$).[17] Expressed at a common reference temperature T^0, each melting process is further characterized by its specific standard free energy change $\Delta G^0_m = \Delta H^0_m - T^0\Delta S^0_m \approx \Delta H_m - T^0\Delta S_m$, which is further used to compute the standard cohesive free energy density CFED = $\Delta G^0_m/V_{mol}$ (V_{mol} is the molar volume),[18] a parameter estimating the average cohesive forces operating in the solid.[19] Interestingly, CFED were found to be linearly correlated with the melting temperatures for series of association/dissociation processes obeying *H*/*S* compensation (Fig. 2a),[17] a phenomenon at the origin of the use of molar volumes for predicting the melting temperatures of linear alkanes (Fig. 2b).[17] However, the exclusive consideration of linear *H*/*S* correlations limits this predictive model to the exploration of narrow domains of melting temperatures.[17]

Theoretical background

Following the formalism of molecular association proposed by Luo and Sharp,[20] the equilibrium constant $K^{A,B}_{asso}$ associated with the simple binding event shown in eqn (1) can be written as eqn (4), where c^θ is the standard concentration of the reference state (fixed to 1 M in this contribution),[21] $H(r, \Omega)$ is a bonding function depending on the separation (r) and orientation (Ω) of the two partners in the [AB] pair ($H(r, \Omega) = 1$ when the complex [AB] exists and $H(r, \Omega) = 0$ otherwise), $\beta = (k_bT)^{-1}$ stands for the thermal factor and $\omega(r, \Omega)$ is the potential mean force between A and B.[10]

$$K^{A,B}_{asso} = \frac{|[AB]|}{|A||B|} = \frac{c^\theta}{8\pi^2}\int H(r,\Omega)e^{-\beta\omega(r,\Omega)}drd\Omega \qquad (4)$$

Solving eqn (4) within the frame of the van't Hoff isotherm for a non-directional harmonic potential $\omega(r, \Omega) = u^{A,B}_{min} + (\kappa^{A,B}/2)r^2$ operating between A and B, whereby $u^{A,B}_{min}$ is the minimum potential energy and $\kappa^{A,B}$ is the force constant, leads to eqn (5) and (6), where N_{Av} is Avogadro number.[10]

$$\Delta H^{A,B}_{asso}/N_{Av} = u^{A,B}_{min} + \frac{3}{2}k_bT \qquad (5)$$

$$\Delta S^{A,B}_{asso}/N_{Av} = k_b \ln\left[c^{\theta}\left(\frac{2\pi e}{\beta\kappa^{A,B}}\right)^{3/2}\right] \quad (6)$$

Interestingly, the enthalpy change $\Delta H^{A,B}_{asso}$ mainly depends on the magnitude of the interaction energy $u^{A,B}_{min}$, while the entropy change $\Delta S^{A,B}_{asso}$ is controlled by the force constant $\kappa^{A,B}$, the latter term being an estimation of the capacity of the bound system to gain residual degrees of freedom. The development of the harmonic potential at the minimum of a standard Lennard-Jones potential $V_{L\text{-}J}$ shows that the absolute minimum energy of the attractive well depth corresponds to $u^{A,B}_{min}$ when the equilibrium A···B separation amounts to $2^{1/6}r^0$ (r^0 is the critical intermolecular A···B distance at which the interaction potential is zero: $V_{L\text{-}J}(r = r^0) = 0$, see Fig. S1 in the ESI†).[6d] Consequently, the total energy of the harmonic oscillator for the special motion amplitude $(2^{1/6}r^0 - r^0)$ exactly corresponds to the well depth $u^{A,B}_{min}$ and eqn (7) results.[6d]

$$-u^{A,B}_{min} = \frac{\kappa^{A,B}\left[r_0\left(1-2^{1/6}\right)\right]^2}{2} \Rightarrow \kappa^{A,B} = -\frac{2}{\left(1-2^{1/6}\right)^2 (r_0)^2}u^{A,B}_{min} = -fu^{A,B}_{min} \quad (7)$$

For a minor structural perturbation affecting a series of A and B partners, the minimum contact distance r_0 is constant within the resulting [AB] pairs and Ford's model (eqn (7), right-hand side) predicts that the force constants $\kappa^{A,B}$ (which affects the entropy changes, eqn (6)) are linearly correlated with the potential well depths $u^{A,B}_{min}$ (which measures the enthalpy change, eqn (5)). Since the coefficient $f = 2/(1 - 2^{1/6})^2(r_0)^2$ is positive, a larger cohesive energy between A and B in the [AB] pair (*i.e.* $u^{A,B}_{min}$ and $\Delta H^{A,B}_{asso}$ become more negative) produces an increase in the force constant $\kappa^{A,B}$, hence in the mean vibrational frequency in the deeper potential.[6d,10] Since $\Delta S^{A,B}_{asso}/N_{Av} \propto -3/2 \ln[\kappa^{A,B}]$ in eqn (6), larger $\kappa^{A,B}$ induces more negative association entropies and H/S compensation occurs. This model is nothing but the Einstein model for crystals,[16,18b,22] from which Lindemann postulated that the melting of a solid occurs when the amplitude of the atomic thermal vibrations reaches some critical fraction of the equilibrium lattice spacing.[23] Introducing eqn (7) into eqn (5) provides a simple correlation between the enthalpy change of the association process and the force constant in the bound state (eqn (8); $R = k_b N_{Av}$ is the ideal gas constant). Further introduction into eqn (6) gives the searched (logarithmic) dependence between $\Delta H^{A,B}_{asso}$ and $\Delta S^{A,B}_{asso}$ (eqn (9)).[6d]

$$\frac{\Delta H^{A,B}_{asso}}{N_{Av}} = \frac{-\kappa^{A,B}}{f} + \frac{3}{2}k_b T \Rightarrow \kappa^{A,B} = \frac{f}{N_{Av}}\left(\frac{3}{2}RT - \Delta H^{A,B}_{asso}\right) \quad (8)$$

$$\Delta S^{A,B}_{asso} = R\left[\ln\left(c^{\theta}\right) + \frac{3}{2}\ln\left(\frac{2\pi eRT}{f}\right) - \frac{3}{2}\ln\left(\frac{3}{2}RT - \Delta H^{A,B}_{asso}\right)\right] \quad (9)$$

Its application to the melting of the A_n assembly shown in eqn (3) requires $\Delta H_m = -\Delta H_{asso}$ and $\Delta S_m = -\Delta S_{asso}$, and eqn (10) eventually results

$$\Delta S_m = R\left[\frac{3}{2}\ln\left(\frac{3}{2}RT + \Delta H_m\right) - \ln\left(c^{\theta}\right) - \frac{3}{2}\ln\left(\frac{2\pi eRT}{f}\right)\right] \quad (10)$$

Applied to the melting of a series of similar compounds,[17] the force constant $\kappa^{A,B}$ can be approximated by a first-order Taylor series around its average magnitude $\kappa^{A,B}_0$, and $\ln\left(\frac{3}{2}RT + \Delta H_m\right)$ in eqn (10) can be replaced with $\ln\left(\frac{3}{2}RT + \Delta H_{m,0}\right) + (\Delta H_m - \Delta H_{m,0})\Big/\left(\frac{3}{2}RT + \Delta H_{m,0}\right)$, where $\Delta H_{m,0}$ is the average melting enthalpy in the series.[6d] However, the rapid divergence of the logarithmic function from a linear approximation restricts the use of linear H/S compensation within this model to a narrow thermodynamic range of melting processes. In this contribution, we propose to improve the predictive capacity of the latter thermodynamic model *via* a thorough investigation of the melting processes occurring in metals, in various organic compounds and in inorganic oxides.

Results and discussion

Modelling *H*/*S* compensation

Thanks to Yaws' efforts for gathering melting enthalpies and entropies (Fig. 3),[24] we were able to select six families of compounds, linear alkanes (Table S1†), linear alkanoic acids (Table S2†), organosilanes (Table S3†), lanthanide metals (Table S4†), transition metals (Table S5†) and transition metal oxides (Table S6†), for which (i) the internal cohesion forces result from various types of intermolecular interactions (permanent and/or induced electric multipolar, H-bonds, covalency) and (ii) the melting temperatures span a broad domain. Assuming the justified approximation that ΔH_m and ΔS_m are essentially constant over a reasonable temperature range around a reference temperature T^0 taken as the average melting temperature within each series (Tables S1–S6 in the ESI†),[17] the experimental ΔS_m *versus* ΔH_m plots of the six individual series were fitted with Ford's model by tuning f in eqn (10), but only a poor match

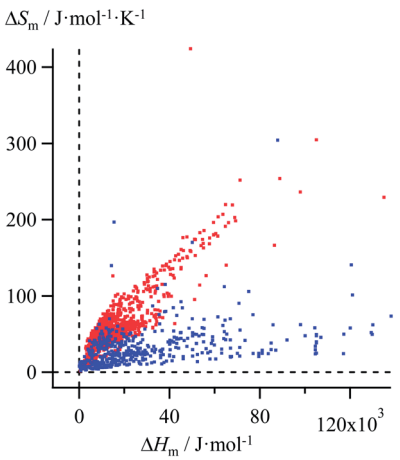

Fig. 3 Plot of melting entropies ΔS_m *versus* melting enthalpies ΔH_m for 764 randomly selected organic compounds (red markers) and 230 inorganic compounds (blue markers).[24]

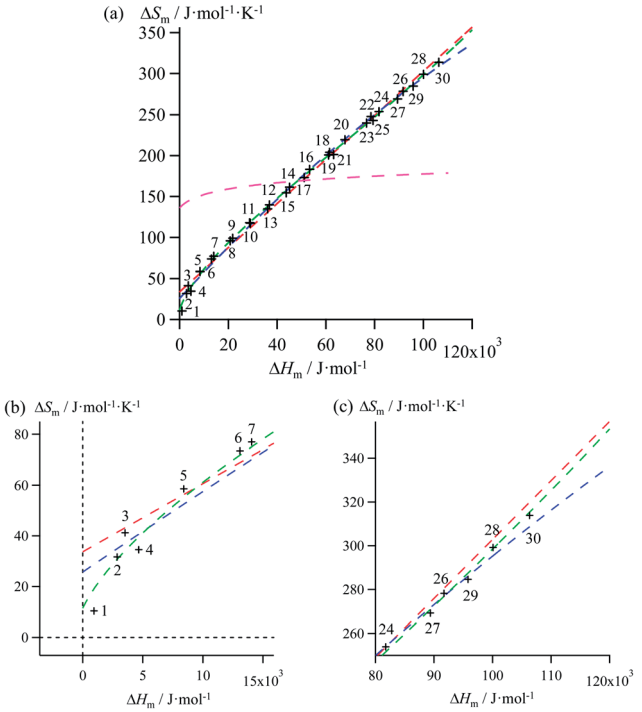

Fig. 4 (a) Full representation, (b) low enthalpy inset and (c) high enthalpy inset for plots of melting entropies ΔS_m *versus* melting enthalpies ΔH_m in linear alkanes C_nH_{2n+2} (n = 1–30) and fitted unconstrained correlations using (i) Ford's approach (eqn (10), magenta trace), (ii) a linear *H*/*S* function (red trace), (iii) a parabolic *H*/*S* function (blue trace) or (iv) a reciprocal Hill plot (green trace).

results (magenta trace in Fig. 4 for linear alkanes and in Fig. S2–S6 for the five other series in the ESI†).

Mathematically speaking, the fitting process is logically improved by the stepwise consideration of additional tuneable parameters according to the following order: Ford's model (eqn (10), one tuneable parameter, magenta traces) < linear fits ($\Delta S_m = a + b\Delta H_m$, two tuneable parameters, red traces) < parabolic fits ($\Delta S_m = a + b\Delta H_m + c(\Delta H_m)^2$, three tuneable parameters, blue traces) < reciprocal Hill fits ($\Delta S_m = a[(\Delta H_m - b)/(\Delta H_m + c)]^d$, four tuneable parameters, green traces; Fig. 4 and S2–S6 and Tables 1 and S7–S11)†. The use of linear and parabolic fits is reminiscent of the use of first-order, respectively second-order Taylor polynomials for approaching eqn (10).[17] Higher-order Taylor series are precluded by the well-known Runge's phenomenon, which strongly limits the approximation of logarithmic mapping by using power polynomials of increasing orders.[25] On the contrary, the use of a Hill function has no mathematical justification for fitting logarithmic plots, but its stability over a large enthalpy range appeared to be a considerable advantage for fitting *H*/*S* compensation (*vide infra*). A simple look at Fig. 3 indicates that $\Delta S_m \rightarrow 0$ when $\Delta H_m \rightarrow 0$ for melting processes recorded at normal pressure (in other words, the melting temperature $T_m = \Delta H_m/\Delta S_m$ does not diverge for $\Delta S_m \rightarrow 0$),[26] a boundary condition which is not satisfied by the fitting traces collected in Fig. 4 and S2–S6 (ESI†). Including the latter constraint into *H*/*S* compensation results in the loss of one degree of freedom by fixing one parameter during the fitting process (Tables 1 and S7–S11,† column 1). Consequently, Ford's approach lacks of acceptable correlation (magenta traces in Fig. 5 and S7–S11,† no tuneable parameter), while linear approximations (red traces in Fig. 5 and S7–S11,† one tuneable parameter, $\Delta S_m = b\Delta H_m$) are dismissed because only a single melting temperature $T_m = b^{-1}$ is tolerated along the complete series of compounds.

Therefore, among the four mathematical functions selected for extending the logarithmic *H*/*S* dependence suggested by the simple Ford's model, only parabolic (blue traces, two tuneable parameters) and Hill (green traces, three tuneable parameters) plots provide satisfying fitted traces compatible with the inclusion of the extra boundary condition $\Delta S_m \rightarrow 0$ when $\Delta H_m \rightarrow 0$ (Fig. 5 and S7–S11, Tables 1 and S7–S11, ESI†).[6a]

Cohesive free energy densities and three-dimensional ΔH_m, ΔS_m, V_{mol} plots

Taking Trouton's rule into account for the vaporization of liquids,[27] Hildebrand introduced the concept of cohesion energy density CED = $(\Delta H_v - RT)/V_{mol}$ for estimating the average cohesive forces operating within liquids and for predicting their vaporization temperatures (ΔH_v is the vaporization enthalpy).[19] In absence of valuable alternative to Trouton's rule fixing the melting entropy in solids,[18] we have resorted to standard melting Gibbs free energy $\Delta G^0_m = \Delta H_m - T^0\Delta S_m$ computed at a

Table 1 Entropy–enthalpy correlations fitted for linear alkanes C_nH_{2n+2} (n = 1–30)[a]

Function	f/m^{-2}	a	b	c	d
Unconstrained					
Eqn (10)	$6(7) \times 10^5$	—	—	—	—
$\Delta S_m = a + b\Delta H_m$	—	33(2)	$2.69(4) \times 10^{-3}$	—	—
$\Delta S_m = a + b\Delta H_m + c(\Delta H_m)^2$	—	26(2)	$3.2(1) \times 10^{-3}$	$-5(1) \times 10^{-9}$	—
$\Delta S_m = a[(\Delta H_m - b)/(c - \Delta H_m)]^d$	—	$4.9(8) \times 10^2$	$-7(8) \times 10^2$	$3.3(5) \times 10^5$	$6.2(3) \times 10^{-1}$
Constrained: $\Delta S_m \rightarrow 0$ when $\Delta H_m \rightarrow 0$					
Eqn (10)	11.39	—	—	—	—
$\Delta S_m = a + b\Delta H_m$	—	0	$3.17(6) \times 10^{-3}$	—	—
$\Delta S_m = a + b\Delta H_m + c(\Delta H_m)^2$	—	0	$4.2(2) \times 10^{-3}$	$-1.3(2) \times 10^{-8}$	—
$\Delta S_m = a[(\Delta H_m - b)/(c - \Delta H_m)]^d$	—	$4.5(4) \times 10^2$	0	$3.0(3) \times 10^5$	$5.9(2) \times 10^{-1}$

[a] Units used for polynomial fits: a/J mol^{-1} K^{-1}, b/K^{-1} and c/J^{-1} mol K^{-1}. Units used for reciprocal Hill fits: a/J mol^{-1} K^{-1}, b and c in J mol^{-1}.

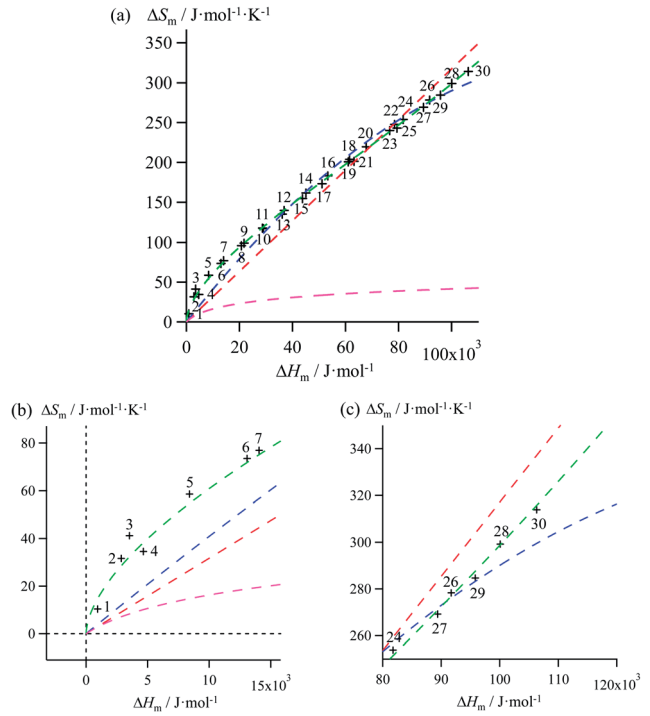

Fig. 5 (a) Full representation, (b) low enthalpy inset and (c) high enthalpy inset for plots of melting entropies ΔS_m *versus* melting enthalpies ΔH_m in linear alkanes C_nH_{2n+2} (n = 1–30) and fitted constrained correlations including $\Delta S_m \rightarrow 0$ when $\Delta H_m \rightarrow 0$ and using (i) Ford's approach (eqn (10), magenta trace), (ii) a linear *H*/*S* function (red trace), (iii) a parabolic *H*/*S* function (blue trace) or (iv) a reciprocal Hill plot (green trace).

reference temperature T^0 for estimating the standard cohesive free energy densities CFED = $\Delta G^0_m/V_{mol}$ along each homogeneous series of compounds (Tables S1–S6, ESI†). We are aware that the melting enthalpies (ΔH_m) and entropies (ΔS_m) are indeed collected at different temperatures for each compound (*i.e.* at T_m) but their dependence on temperature is limited,[17] and the choice of a reference temperature T^0 around the center of each series obeying *H*/*S* compensation is thus acceptable for computing ΔG^0_m. The experimental linear correlations observed between CFED and the associated melting temperatures T_m in Fig. 6 provide eqn (11), which interconnects ΔH_m, ΔS_m and V_{mol} within each series (note that $T_m = \Delta H_m/\Delta S_m$)

$$\text{CFED} = \frac{\Delta G^0_m}{V_{mol}} = \frac{\Delta H_m - T^0 \Delta S_m}{V_{mol}} = \lambda T_m + \mu \qquad (11)$$

Taken separately, eqn (11) is of limited interest for tuning melting temperatures by molecular design since only the molar volume V_{mol} can be easily computed for unknown compounds,[28] while satisfying estimations and/or modelling of melting

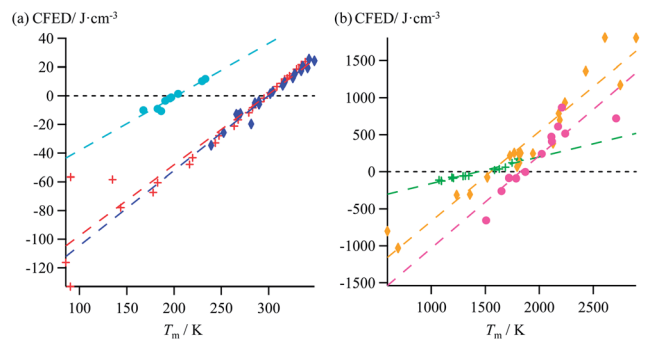

Fig. 6 Plots of standard cohesion free energy densities (CFED) *versus* the melting temperature (T_m) for (a) linear alkanes (red trace), linear alkanoic acids (dark blue trace) and organosilanes (light blue trace), and (b) lanthanide metals (green trace), transition metals (orange trace) and transition metal oxides (magenta trace).

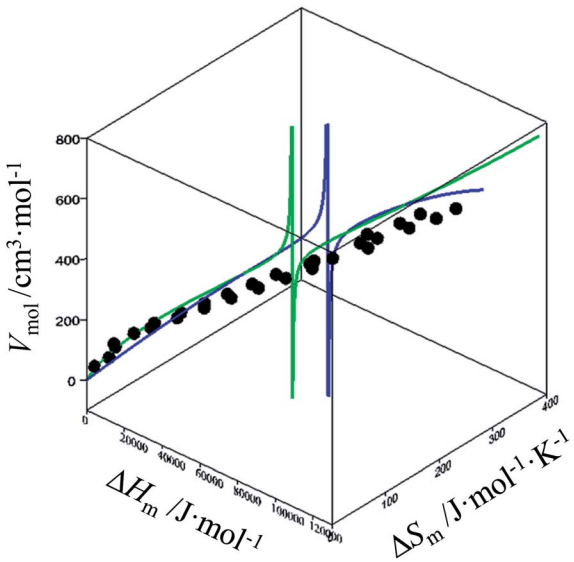

Fig. 7 Three-dimensional V_{mol}, ΔH_m, ΔS_m plot for linear alkanes fitted with a parabolic *H*/*S* function (blue trace) or a reciprocal Hill plots (green trace). An asymptotic behaviour is expected to occur when the melting temperature approaches the selected reference temperature T^0 = 298.15 K.

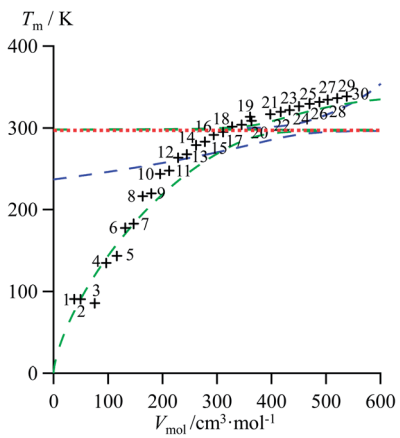

Fig. 8 Correlations between molar volumes V_{mol} and melting temperatures T_m for linear alkanes C_nH_{2n+2} (n = 1–30) fitted using a parabolic *H*/*S* function (blue trace) or a reciprocal Hill plots (green trace). The horizontal dotted red trace corresponds to the asymptotical behaviour occurring when the melting temperature approaches the selected reference temperature T^0 = 298.15 K.

entropies or enthalpies are difficult.[29] However, the consideration of H/S compensations operating in each series (Fig. 5 and S7–S11, ESI†) provides a correlation $\Delta S_m = g_i(\Delta H_m)$ which can be introduced into eqn (11) to give eqn (12) when one reminds that $T_m = \Delta H_m/\Delta S_m = \Delta H_m/g_i(\Delta H_m)$ (g_i represents either a parabolic or a reciprocal Hill function).

$$g_i(\Delta H_m)[\Delta H_m - T^0 g_i(\Delta H_m) - V_{mol}\mu] - \lambda V_{mol}\Delta H_m = 0 \quad (12)$$

For quadratic fits, $\Delta S_m = g_{quadra}(\Delta H_m) = b\Delta H_m + c(\Delta H_m)^2$ and eqn (12) corresponds to a polynomial, which can be solved to give an estimation of the melting enthalpy ΔH_m as soon as the molar volumes V_{mol} of a target compound belonging to the series is at hand. The associated melting entropy ΔS_m immediately results from H/S correlation. The same procedure holds when using reciprocal Hill fits characterized by $\Delta S_m = g_{Hill}(\Delta H_m) = a[\Delta H_m/(\Delta H_m + c)]^d$. The quality of the correlations can be estimated in the three-dimensional V_{mol}, ΔH_m, ΔS_m plots for each series (Fig. 7 and S12–S16, ESI†).

As an ultimate step, the combination of melting enthalpies and entropies into the melting temperatures $T_m = \Delta H_m/\Delta S_m$ reduces the dimension of the correlation shown in Fig. 7 to give an easy-manageable T_m *versus* V_{mol} plot (Fig. 8 and S17–S21, ESI†). The careful inspection of the latter two-dimensional plots indicate that, for any series under investigation, reciprocal Hill functions provide the best fits.

Combination of *H/S* compensation with linear cohesive free energy densities (CFED) for predicting the melting temperatures of substituted lipophilic cyanobiphenyls

Lipophilic cyanobiphenyls with variable lengths (*n*-CB) and substitutions (12Me$_m$-CB) have been considered as precursors for inducing liquid crystalline mesophases (Fig. 9a, Table S12,

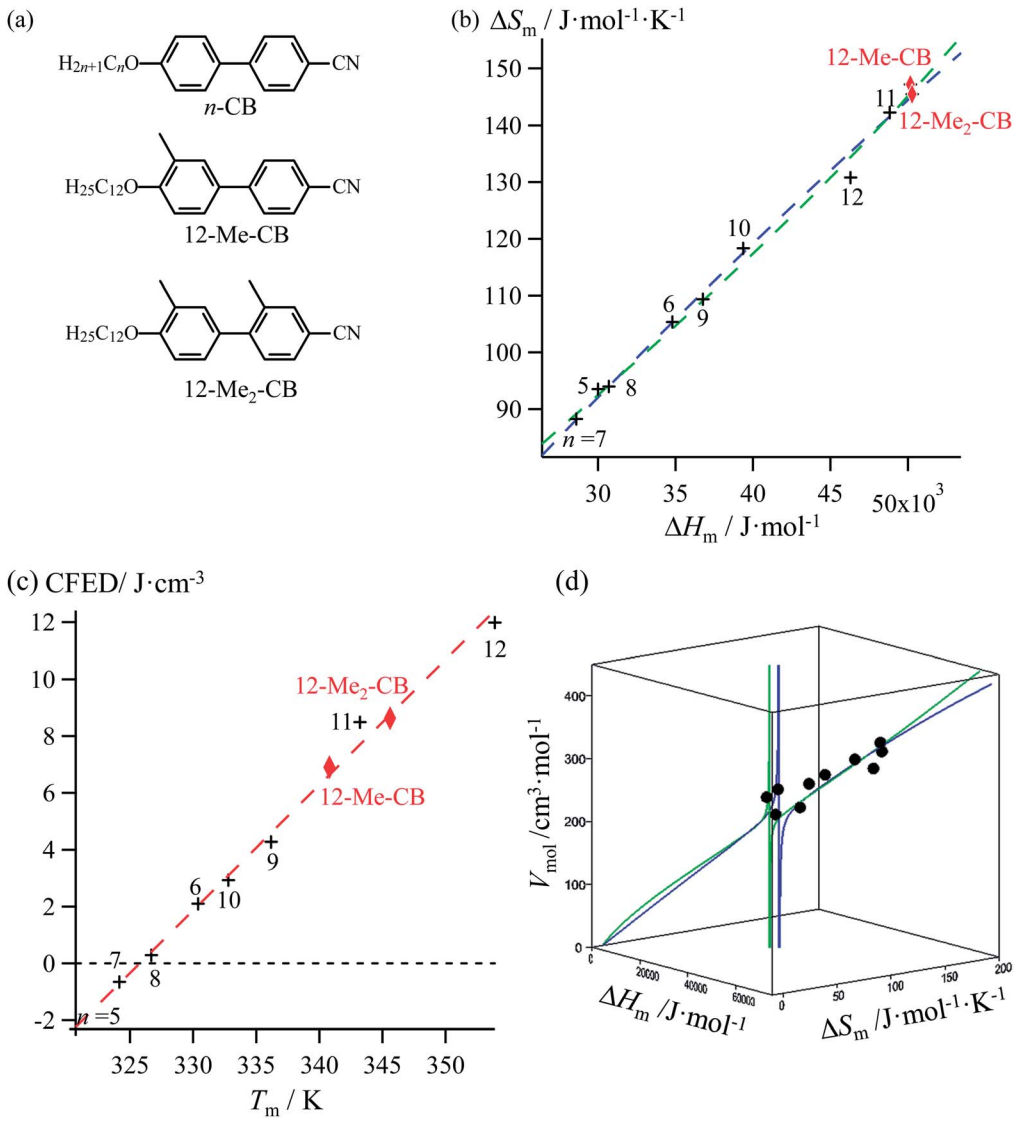

Fig. 9 (a) Chemical structures of substituted cyanobiphenyls with associated plots corresponding to (b) melting entropy *versus* melting enthalpy changes, (c) cohesion free energy densities (CFED) *versus* the melting temperature (T_m) and (d) three-dimensional V_{mol}, *versus* ΔH_m and ΔS_m fitted with a parabolic H/S function (blue trace) or a reciprocal Hill function (green trace). Reference temperature $T^0 = 325.92$ K.

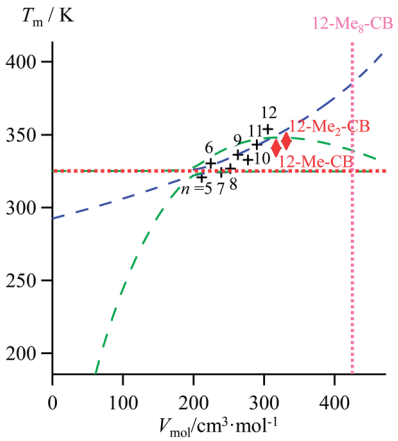

Fig. 10 Correlations between molar volumes V_{mol} and melting temperatures T_m for substituted lipophilic cyanobiphenyls fitted using a parabolic *H*/*S* function (blue trace) or a reciprocal Hill plots (green trace). The horizontal dotted red trace corresponds to the asymptotical behaviour occurring when the melting temperature approaches the selected reference temperature $T^0 = 325.95$ K. The vertical dotted magenta trace shows the predictions obtained for the permethylated cyanobiphenyl 12-Me$_8$-CB.

ESI†).[17] Both constrained quadratic and reciprocal Hill correlations satisfyingly model *H*/*S* compensation along the cyanobiphenyl series (Fig. 9b), which further displays a linear CFED *versus* T_m plot according to eqn (11) (Fig. 9c). The three-dimensional V_{mol}, ΔH_m, ΔS_m plot fitted with eqn (12) confirms the comparable quality of quadratic (blue trace) or Hill (green trace) functions (Fig. 9d). However, the trends predicted beyond the range of available experimental data significantly differ for the quadratic (blue trace) and Hill (green trace) plots, a feature highlighted in the reduced two-dimensional T_m *versus* V_{mol} plot (Fig. 10).[30]

The ultimate step of our model offers the opportunity to predict the melting temperature for the unknown permethylated 4′-(dodecyloxy)-4-cyanobiphenyl compound (12-Me$_8$-CB), for which a molecular volume of 688.5 Å^3, hence a molar volume of $V_{mol} = N_{Av} \times 688.5 \times 10^{-24} = 414.2$ cm^3 mol^{-1} can be estimated.[17,28] Depending on the choice of the fitting curve used for modelling *H*/*S* compensation, an increase (quadratic fit) or a stagnation (Hill fit) of the melting temperature is expected, and one can therefore predicts T_m (12-Me$_8$-CB) = 380.5 K based on the quadratic fit and 340.7 K based on the Hill fit (Fig. 10). Since the experimental number of methyl groups bound to the cyanobiphenyl core in 12-Me$_m$-CB is currently limited to $m = 2$,[17] no definitive preference between quadratic and Hill predictions can be set. However, the stagnation of the melting temperature detected upon successive methylation (T_m (12-CB) ≥ T_m (12-Me-CB) ≈ T_m (12-Me$_2$-CB) in Fig. 10) has been confirmed by the systematic preparation of all the possible regioisomers of 12-Me-CB (4 isomers, average melting temperature T_m (monomethyl-CB) = 326(11) K), and those of 12-Me$_2$-CB (4 isomers with one methyl group connected to each aromatic group, average melting temperature T_m (dimethyl-CB) = 327(16) K).[17] This trend represents a strong support in favor of the Hill plot as the best predictive tool within this novel series, in line with the previous analysis of linear alkane and alkanoic acids, organosilanes, lanthanide metals, transition metals and transition metal oxides.

Conclusion

The non-directional Ford's approach uses a single harmonic potential with a unique minimum contact distance for catching any intermolecular interaction. It predicts that, for a series of binding reactions involving structurally similar partners, the thermodynamic of association/dissociation is dominated by *H*/*S* compensation and logarithmic ΔS *versus* ΔH dependences are expected. Applied to the melting processes occurring in six (arbitrarily selected) sets of chemical compounds, this rough model justifies the emergence of *H*/*S* compensation, but it fails in reproducing accurate trends because the modelling of the intermolecular interactions operating in solid with the help of a single harmonic potential is a too big oversimplification. Increasing the number of degrees of freedom for approaching *H*/*S* correlations restores satisfying fits when using linear or quadratic polynomials, or reciprocal Hill functions. The inclusion of the boundary condition $\Delta S_m \rightarrow 0$ when $\Delta H_m \rightarrow 0$ recuses linear *H*/*S* correlations and only quadratic or Hill plots are able to give satisfying ΔS_m *versus* ΔH_m fits. Standard empirical analysis of enthalpy/entropy compensation within the frame of this simple binding thermodynamics stops at this point, and no predictive tool is at hand for estimating the strength of intermolecular interactions and for programming melting temperatures. The additional concept of standard cohesive free energy density (CFED = $\Delta G^0_m/V_{mol}$) and its observed linear correlation with the melting temperatures (eqn (11)) introduces an unprecedented relationship between the molar volume, V_{mol}, a parameter accessible to supramolecular chemists and the correlated melting enthalpies and entropies. For the six different series of compounds selected in this contribution, *i.e.* linear alkanes, linear alkanoic acids, organosilanes, lanthanide metals, transition metals and transition metal oxides, the ultimate reduced T_m *versus* V_{mol} plots satisfyingly reproduce the experimental data. We notice that the use of reciprocal Hill plots provide the best fits for *H*/*S* correlations in melting processes, and its application for rationalizing melting temperatures recently determined for substituted cyanobiphenyls provides reasonable predictions for currently unknown compounds in the series.

Experimental

The mathematical analyses were performed by using Igor Pro® (WaveMetrics Inc.) and Excel® (Microsoft) softwares.

Acknowledgements

Financial support from the Swiss National Science Foundation is gratefully acknowledged.

References and notes

1 (*a*) M. Mammen, S.-K. Choi and G. M. Whitesides, *Angew. Chem., Int. Ed.*, 1998, **37**, 2754–2794; (*b*) A. Mulder, J. Huskens and D. N. Reinhoudt, *Org. Biomol. Chem.*, 2004, **2**, 3409–3424; (*c*) M. T. Rodgers and P. B. Armentrout, *Acc. Chem. Res.*, 2004, **37**, 989–998; V. M. Krishnamurthy, B. R. Bohall, V. Semetey and G. M. Whitesides, *J. Am. Chem. Soc.*, 2006, **128**, 5802–5812.

2 (*a*) L. Cademartiri, K. J. M. Bishop, P. W. Snyder and G. A. Ozin, *Philos. Trans. R. Soc., A*, 2012, **370**, 2824–2847; (*b*) C.-A. Palma, M. Cecchini and P. Samori, *Chem. Soc. Rev.*, 2012, **41**, 3713–3730; (*c*) J. Li, P. Nowak and O. Sijbren, *J. Am. Chem. Soc.*, 2013, **135**, 9222–9239.

3 (*a*) J. D. Badjic, A. Nelson, S. J. Cantrill, W. B. Turnbull and J. F. Stoddart, *Acc. Chem. Res.*, 2005, **38**, 723–732; (*b*) H.-J. Schneider, *Angew. Chem., Int. Ed.*, 2009, **48**, 3924–3977; (*c*) C. Piguet, *Chem. Commun.*, 2010, **46**, 6209–6231; (*d*) R. Chakrabarty, P. S. Mukherjee and P. J. Stang, *Chem. Rev.*, 2011, **111**, 6810–6918.

4 T. Engel and P. Reid, *Physical Chemistry*, Pearson Benjamin Cummings, San Francisco, 2006, pp. 113–122.

5 (*a*) M. S. Searle, M. S. Westwell and D. H. Williams, *J. Chem. Soc., Perkin Trans. 2*, 1995, 141–151; (*b*) C. Neal, A. Starace and M. Jarrold, *Phys. Rev. B: Condens. Matter Mater. Phys.*, 2007, **76**, 054113.

6 (*a*) L. Liu and Q.-X. Guo, *Chem. Rev.*, 2001, **101**, 673–695; (*b*) K. Sharp, *Protein Sci.*, 2001, **10**, 661–667; (*c*) E. B. Starikov and B. Norden, *J. Phys. Chem. B*, 2007, **111**, 14431–14435; (*d*) C. Piguet, *Dalton Trans.*, 2011, **40**, 8059–8071.

7 (*a*) J. E. Leffler, *J. Org. Chem.*, 1955, **20**, 1202–1231; (*b*) D. H. Williams, E. Stephens, D. P. O'Brien and M. Zhou, *Angew. Chem., Int. Ed.*, 2004, **43**, 6596–6616; (*c*) D. H. Leung, R. G. Bergman and K. N. Raymond, *J. Am. Chem. Soc.*, 2008, **130**, 2798–2805.

8 (*a*) R. Lumry, *Methods Enzymol.*, 1995, **259**, 628–720; (*b*) A. Cornish-Bowden, *J. Biosci.*, 2002, **27**, 121–126.

9 K. F. Freed, *J. Phys. Chem. B*, 2011, **115**, 1689–1692.

10 (*a*) D. M. Ford, *J. Am. Chem. Soc.*, 2005, **127**, 16167–16170; (*b*) D. M. Ford, *Adsorption*, 2005, **11**, 271–277.

11 V. S. Shaikh, S. S. Terdale, A. Ahamad, G. R. Gupta, D. H. Dagade, D. G. Hundiwale and K. J. Patil, *J. Phys. Chem. B*, 2013, **117**, 16249–16259.

12 E. B. Starikov and B. Norden, *J. Phys. Chem. B*, 2009, **113**, 4698–4707.

13 T. B. Jensen, E. Terazzi, K. Buchwalder, L. Guénée, H. Nozary, K. Schenk, B. Heinrich, B. Donnio, D. Guillon and C. Piguet, *Inorg. Chem.*, 2010, **49**, 8601–8619.

14 (*a*) B. M. Castellano and D. K. Eggers, *J. Phys. Chem. B*, 2013, **117**, 8180–8188; (*b*) E. Terazzi, A. Zaïm, B. Bocquet, J. Varin, L. Guénée, T. Dutronc, J.-F. Lemonnier, S. Floquet, E. Cadot, B. Heinrich, B. Donnio and C. Piguet, *Eur. J. Inorg. Chem.*, 2013, 3323–3333.

15 (*a*) E. Fisicaro, C. Compari and A. Braibanti, *Phys. Chem. Chem. Phys.*, 2004, **6**, 4156–4166; (*b*) J. M. Ward, N. M. Gorenstein, J. Tian, S. F. Martin and C. B. Post, *J. Am. Chem. Soc.*, 2010, **132**, 11058–11070; (*c*) B. Breiten, M. R. Lockett, W. Sherman, S. Fujita, M. Al-Sayah, H. Lange, C. M. Bowers, A. Heroux, G. Krilov and G. M. Whitesides, *J. Am. Chem. Soc.*, 2013, **135**, 15579–15584.

16 S. Zamith, F. Chirot and J.-M. L'Hermite, *Europhys. Lett.*, 2010, **92**, 13004.

17 T. Dutronc, E. Terazzi, L. Guénée, K.-L. Buchwalder, A. Spoerri, D. Emery, J. Mareda, S. Floquet and C. Piguet, *Chem.–Eur. J.*, 2013, **19**, 8447–8456.

18 Since Richard's rule only holds for metals, the entropies of melting for organic compounds cannot be taken as constant, and the CFED parameter is thus derived from the free energy change (*a*) G. P. Tiwari, *Met. Sci.*, 1978, **12**, 317–320; (*b*) M. E. Glicksman, *Principle of Solidification*, Springer, New York, 2011, p. 22.

19 (*a*) M. Dunkel, *J. Phys. Chem.*, 1928, **A138**, 42–54; (*b*) J. H. Hildebrand and R. L. Scott, *The Solubility of Nonelectrolytes*, Reinhold Pub Group, New York, 3rd edn, 1950; (*c*) R. F. Fedors, *Polym. Eng. Sci.*, 1974, **14**, 147–154; (*d*) A. F. M. Barton, *Handbook of Solubility Parameters and Other Cohesion Parameters*, CRC Press, 2nd edn, 1991, p. 127.

20 H. B. Luo and K. Sharp, *Proc. Natl. Acad. Sci. U. S. A.*, 2002, **99**, 10399–10404.

21 D. Munro, *Chem. Br.*, 1977, **13**, 100–105.

22 (*a*) A. Einstein, *Ann. Phys.*, 1907, **22**, 180–190; (*b*) D. W. Rogers, *Einstein's other Theory, the Plank–Bose–Einstein Theory of Heat Capacity*, Princeton University Press, New Jersey, 2005.

23 F. A. Lindemann, *Phys. Z.*, 1910, **11**, 609–612.

24 C. L. Yaws, *Yaws Handbook of Thermodynamics and Physical Properties of Chemical Compounds*, Knovel-Elsevier, Norwich New York, 2003.

25 C. Runge, *Zeitschrift für Mathematik und Physik*, 1901, **46**, 224–243.

26 Under critical conditions of pressure, a continuous transition from crystal to melt displaying $\Delta S_m = 0$ and $\Delta V_m = 0$ whilst $\Delta H_m \neq 0$ is theoretically justified. However, no experimental demonstration of this prediction is currently available because of the extreme pressure conditions required for the most promising candidatesA. R. Ubbelohde, *Melting and Crystal Structures*, Clarendon Press, Oxford, 1965, pp. 19–24.

27 Trouton's rule states that the entropy of vaporization for any liquid is almost the same value, about 85–88 J K^{-1} mol^{-1}. Consequently, the vaporization temperature entirely depends on the vaporization enthalpy. F. T. Trouton, *London, Edinburgh Dublin Philos. Mag. J. Sci.*, 1884, **18**, 54–57.

28 The molar volumes $V_{mol} = N_{Av} \times V_{Connolly} \times 10^{-24}$ in cm^3 mol^{-1} are deduced from the Connollyvolumes expressed in $Å^3$. $V_{Connolly}$ are obtained from the building of the Connolly surfaces around the molecular structures of the compounds observed in their crystal structures (when available) or in their gas-phase structures modelled by semi-empirical PM3 method (*a*) M. L. Connolly, *Science*, 1983, **221**, 709–713; (*b*) M. L. Connolly, *J. Appl. Crystallogr.*,

1983, **16**, 548–558; (*c*) J. J. P. Stewart, *J. Comput. Chem.*, 1989, **10**, 209–220; (*d*) J. J. P. Stewart, *J. Comput. Chem.*, 1989, **10**, 221–264.

29 (*a*) A. R. Katritzky, U. Maran, M. Karelson and V. S. Lobanov, *J. Chem. Inf. Comput. Sci.*, 1997, **37**, 913–919, and references therein; (*b*) Y. Tsuchiya, H. Hasegawa and T. Iwatsubo, *J. Chem. Phys.*, 2001, **114**, 2484–2488; (*c*) Y. Tsuchiya, H. Hasegawa and T. Iwatsubo, *Jpn. J. Appl. Phys., Part 1*, 2003, **42**, 6508–6511.

30 For any cyanobiphenyl located close to the asymptote (*i.e.* possessing molar volumes in the 200–260 cm^3 mol^{-1} range), a simple change of the reference temperature provides its unambiguous location on either part of the fitting curve (Fig. S22, ESI†).

